LASER
& PHOTONICS
REVIEWS

Laser Photonics Rev. **8,** No. 5, L76–L80 (2014) / **DOI** 10.1002/lpor.201400057

LETTER
ARTICLE

Abstract Quantum optics plays a central role in the study of fundamental concepts in quantum mechanics, and in the development of new technological applications. Typical experiments employ sources of photon pairs generated by parametric processes such as spontaneous parametric down-conversion and spontaneous four-wave-mixing. The standard characterization of these sources relies on detecting the pairs themselves and thus requires single photon detectors, which limit both measurement speed and accuracy. Here it is shown that the two-photon quantum state that would be generated by parametric fluorescence can be characterised with unprecedented spectral resolution by performing a classical experiment. This streamlined technique gives access to hitherto unexplored features of two-photon states and has the potential to speed up design and testing of massively parallel integrated nonlinear sources by providing a fast and reliable quality control procedure. Additionally, it allows for the engineering of quantum light states at a significantly higher level of spectral detail, powering future quantum optical applications based on time-energy photon correlations.

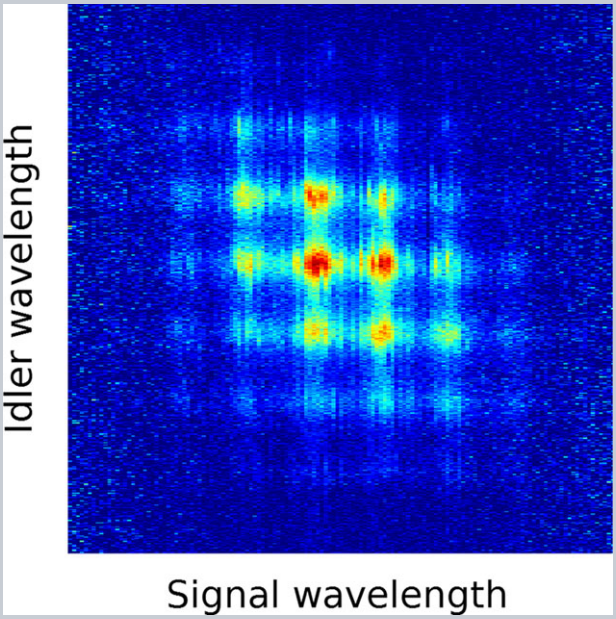

High-resolution spectral characterization of two photon states via classical measurements

Andreas Eckstein[1], Guillaume Boucher[1], Aristide Lemaître[2], Pascal Filloux[1], Ivan Favero[1], Giuseppe Leo[1], John E. Sipe[3], Marco Liscidini[4], and Sara Ducci[1,*]

1. Introduction

One of most utilized strategies to generate quantum correlated photons is exploiting spontaneous parametric down-conversion (SPDC), the spontaneous fission of a "pump" photon into a pair of photons, "signal" and "idler", in a nonlinear medium (see Fig. 1a). In general, the probability of such an event is very small. Thus the quantum state describing the radiation field in the frequency regime of signal and idler is mostly the vacuum state $|0\rangle$, but it also contains a normalized two-photon component

$$|\psi_{\text{pair}}\rangle = \frac{1}{\sqrt{2}} \sum_{\nu,\eta} \iint \mathrm{d}\omega_1 \, \mathrm{d}\omega_2 \, \phi_{\nu,\eta}(\omega_1, \omega_2) \times \hat{\mathrm{a}}^{\dagger}_{\nu}(\omega_1) \hat{\mathrm{a}}^{\dagger}_{\eta}(\omega_2) \, |0\rangle \, . \quad (1)$$

with a small probability amplitude γ; here $|\gamma|^2$ is the probability with which a photon pair is emitted, ν and η label the modes into which the photons are generated, and ω_1 and ω_2 indicate their frequencies. The biphoton wavefunction $\phi_{\nu,\eta}(\omega_1, \omega_2)$ characterizes all properties of the two-photon state, and it describes any quantum correlation between the two emitted photons; $\phi_{\nu,\eta}(\omega_1, \omega_2)$ is determined by the medium in which SPDC occurs, as well as the pumping scheme [1]. In particular, $|\phi_{\nu,\eta}(\omega_1, \omega_2)|^2$ is known as the joint spectral density (JSD), with $|\phi_{\nu,\eta}(\omega_1, \omega_2)|^2 \mathrm{d}\omega_1 \mathrm{d}\omega_2$ being the probability of generating "photon 1" in the mode ν with frequency within $\mathrm{d}\omega_1$ of ω_1, and "photon 2" in the mode η with frequency within $\mathrm{d}\omega_2$ of ω_2.

So far, the JSD has been obtained by performing spectrally resolved single photon coincidence measurements [2–4]. In practice this strategy is constrained by the pair generation probability, which must be much smaller than unity within the time resolution of the single photon detector; otherwise an error would be introduced in the measured spectral correlations by the detection of multiple photon

[1] Laboratoire Matériaux et Phénoménes Quantiques, Université Paris Diderot, Sorbonne Paris Cité, CNRS-UMR 7162, Case courrier 7021, 75205 Paris Cedex 13, France
[2] Laboratoire de Photonique et Nanostructures, CNRS-UPR20, Route de Nozay, 91460 Marcoussis, France
[3] Department of Physics and Institute for Optical Sciences, University of Toronto, 60 St. George Street, Ontario M5S 1A7, Canada
[4] Department of Physics, University of Pavia, Via Bassi 6, I-27100 Pavia, Italy
*Corresponding author: e-mail: sara.ducci@univ-paris-diderot.fr

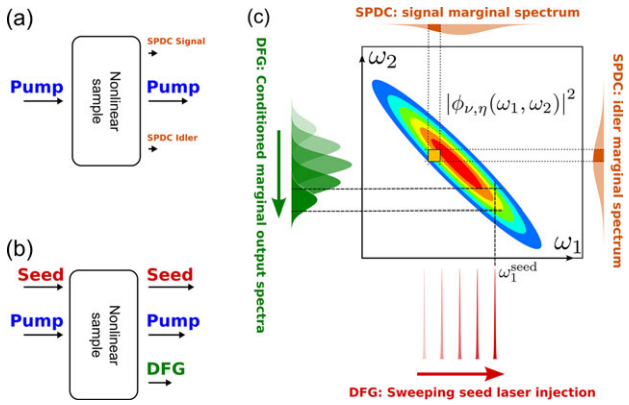

Figure 1 Working principle: (a) In a sample with a second order optical nonlinearity, SPDC converts a photon from the coherent pump pulse into a signal and idler photon pair with some probability. (b) If a coherent "seed" beam is introduced into the nonlinear sample in the mode of either the signal or the idler photon, a DFG process takes place and the conversion rate of pump photons is stimulated and increased by a factor proportional to the seed beam power. (c) Reconstruction of a typical JSD, shared by the SPDC and the DFG process for the same nonlinear sample and the same pump configuration. In the SPDC case, the emitted signal and idler photons are analyzed with spectrometers. By single photon coincidence detection of each spectrometer's transmission, the intensity of a "pixel", corresponding to the joint transmission of both spectrometers' filter characteristics, is measured. The whole JSD can be reconstructed after collecting a sufficient number of events. In the DFG case, a narrow-band seed laser beam at frequency ω_1^{seed} stimulates the emission of a spectrally pre-conditioned coherent output beam in the idler mode. This spectrum is proportional to a "slice" of the JSD corresponding to the injected wavelength (see Eq. 2). Sweeping the seed wavelength allows the reconstruction of the JSD.

pairs. Moreover, after the detection event each single photon detector has to be re-set to an operational state; this results in a deadtime τ_D, which limits the maximally detectable coincidence rate to τ_D^{-1}. These constraints lead to unavoidable limitations in the spectral resolution with which the JSD can be determined. On one hand, a large number of coincidences is required for reasonably low relative errors, demanding long integration times. On the other hand, short experimental runs are desirable to minimize any drift in the experimental conditions and to allow the characterization of a large number of sources. Both of these requirements cannot be satisfied simultaneously, and so the development of convenient characterization strategies for quantum correlated photons, necessary for the emergence of advanced quantum optical applications in integrated devices [5–10], remains an outstanding technological challenge.

An alternative approach can be envisioned by recalling that, while SPDC can be described only in the framework of quantum theory, it can be viewed as difference frequency generation (DFG) in the quantum limit. Indeed, in DFG the conversion of pump photons to signal and idler pairs is stimulated by a seed beam, so SPDC can be considered as a DFG process stimulated by vacuum power fluctuations [11]. The existence of a corresponding classical process naturally prompts one to question if it is possible to gain information about the quantum process by investigating only its classical analog. In the past, DFG has been used to determine the phase-matching function of SPDC sources [12, 13]. It has also been experimentally demonstrated that seeded four-wave mixing (FWM) can be used to directly determine the number of pairs that would be generated by spontaneous FWM in ring resonators [14]. Theoretical studies have shown that DFG can be similarly used to determine the number of pairs that would be generated by SPDC, both in ring resonators and in other structures such as waveguides [11]. In another context, DFG has been exploited for the realization of quantum cloning [15].

In this letter we extend this classical-quantum connection even further, and demonstrate experimentally that quantum correlations of photon pairs that would be generated by SPDC can be investigated through measurements of the corresponding DFG process [16]. Besides the intriguing fundamental aspect of this result, we show that our approach makes it possible to achieve an outstanding spectral resolution and increase data acquisition rates well beyond the state-of-the-art for spectrally resolved coincidence measurements [17, 18]. Finally, as one moves from SPDC to DFG, the increase of the generated output beam intensity by several orders of magnitude allows the replacement of single photon detectors with an optical spectrum analyzer (OSA), a widely available general purpose instrument.

The strategy we employ is based on the fact that, provided the same pumping scheme, the biphoton wavefunction $\phi_{\nu,\eta}(\omega_1, \omega_2)$ that *would be relevant* in SPDC plays the role of the response function of the structure that characterizes the generation of the stimulated light by DFG [16]. This is due to the fact that SPDC and DFG share the same phasematching configuration and pump spectrum and thus the same spectral correlation function, as indicated in Fig. 1. In particular, the average number of photons stimulated in the mode η with energy between ω_2 and $\omega_2 + \delta\omega_2$ by a coherent seeding beam exiting the system in mode ν and having energy centered at ω_1 with a width of $\delta\omega_1$ can be written as

$$\begin{aligned}
&\langle \hat{a}_\eta^\dagger(\omega_2)\hat{a}_\eta(\omega_2)\rangle_{B_\nu(\omega_1)}\,\delta\omega_2 \\
&\quad\approx 2|B_\nu(\omega_1)|^2|\gamma|^2|\phi_{\nu,\eta}(\omega_1,\omega_2)|^2\delta\omega_2\delta\omega_1 \\
&\quad\equiv |B_\nu(\omega_1)|^2\,\langle \hat{a}_\eta^\dagger(\omega_2)\hat{a}_\eta(\omega_2)\hat{a}_\nu^\dagger(\omega_1)\hat{a}_\nu(\omega_1)\rangle\,\delta\omega_2\delta\omega_1 \qquad (2)
\end{aligned}$$

where $|B_\nu(\omega_1)|^2$ is the average number of photons in the coherent seeding beam, and $\langle \hat{a}_\eta^\dagger(\omega_2)\hat{a}_\eta(\omega_2)\hat{a}_\nu^\dagger(\omega_1)\hat{a}_\nu(\omega_1)\rangle$ $\delta\omega_2\delta\omega_1$ is the average number of pairs generated within $\delta\omega_2$ and $\delta\omega_1$, by SPDC. Hence, Eq. 2 links the intensity of the signal stimulated via DFG (shown in Fig. 3) to the number of coincidences given by the photon pairs generated via SPDC in the corresponding experiment (Fig. 2). Thus, by scanning the coherent seeding beam over the full spectrum in a DFG experiment (see Fig. 1), it is possible to obtain the JSD, $|\phi_{\nu,\eta}(\omega_1, \omega_2)|^2$, that one would extract from

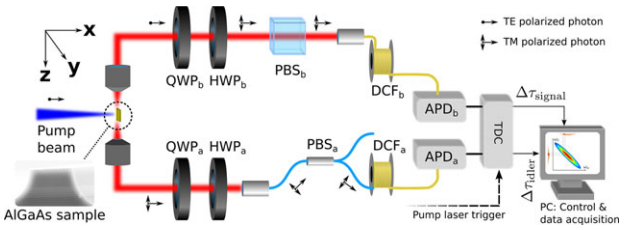

Figure 2 Sketch of the experimental setup for SPDC-based spectral correlation measurements. A pump pulse incident from the top of the semiconductor device leads to the creation of counterpropagating pairs of signal and idler photons in the waveguide. One of the two possible type II phase-matched processes is selected with polarization optics (HWP$_{a/b}$, PBS$_{a/b}$) and two fiber single photon spectrometers [4] are used to analyze signal and idler photon. By introducing high group velocity dispersion with the fiber spools DCF$_{a/b}$, the arrival time of each photon at the avalanche photo-diodes APD$_{a/b}$ relative to the pump laser's electrical trigger signal reveals the photon frequency and is recorded by a personal computer via a time-to-digital converter (TDC).

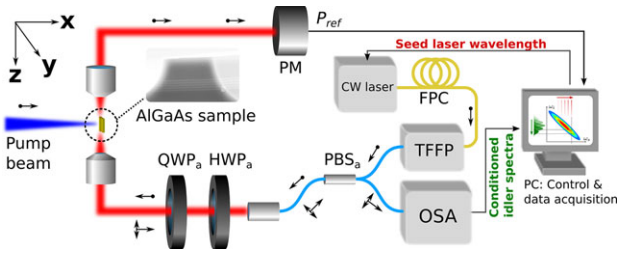

Figure 3 Sketch of the experimental setup for DFG-based spectral correlation measurements. Besides the pump pulse injected as in the SPDC experiment shown in Fig. 2, we inject a CW seed laser beam into the signal mode of the waveguide. Its polarization, adjusted by fiber polarization controller FPC and filtered by PBS$_a$, is used to select the same type II process as in the SPDC experiment. The transmitted seed laser power P_{ref} is measured by the powermeter PM. The tunable, fibered Fabry-Perot filter TFFP is used for spectral clean-up of the seed laser line. The backward emitted DFG beam has the same beam path as the seed beam, but has opposite polarization and propagation direction. The fiber integrated PBS$_a$ is therefore used as a combiner/splitter for both beams to retrieve the DFG output and guide it to an optical spectrum analyzer (OSA).

coincidence measurements in the corresponding SPDC experiment (i.e., without seed). Finally, Eq. 2 tells us that the signal measured in the DFG experiments will be essentially $|B_\nu(\omega_1)|^2$ times the one measured in the corresponding coincidence measurement, and thus several orders of magnitude larger.

2. Experimental results

To demonstrate the advantages of our characterization technique, we experimentally compared SPDC and DFG-based frequency correlation characterizations of an integrated quantum light source: a picosecond-pulse-pumped AlGaAs ridge waveguide in a transverse pump configuration, in which an integrated microcavity with a resonance at the frequency of the pump pulse enhances [13] the emission of counterpropagating photon pairs from two simultaneously phase-matched type II SPDC processes [19]. Integrated sources are attracting a considerable interest for their flexibility and the possibility of mass production, but these sources are also particularly challenging to investigate.

In the SPDC experiment (Fig. 2) we use a fiber spectrometer [4] to reconstruct the JSD by collecting one photon pair at a time. When the detectors indicate the arrival of both a signal and idler photon originating from the same trigger pulse, the corresponding pair of signal/idler arrival times is added to a joint histogram. With a sufficiently large number of collected events this procedure yields the JSD, which is proportional to the coincidence counts plotted in Fig. 4a. Here the spectral resolution is $\Delta\lambda_{SPDC} = 224\,\text{pm}$, limited by the temporal jitter of the single photon detection signal relative to the pump trigger signal.

In the DFG experiment (see Fig. 3) we collect the idler spectrum generated, under the same pumping condition, by sweeping a CW seed beam over the signal bandwidth of the spontaneous process. In accordance with Eq. 2, each preconditioned idler spectrum is proportional to the "slice" of the JSD corresponding to the pairs generated with the signal photon at the wavelength of the CW seed. The measurement result is presented in Fig. 4b. The spectral resolution along the signal axis is determined by the accuracy of the seed laser wavelength (20 pm), while along the idler axis it is given by the OSA resolution (20 pm).

From a simple visual comparison of Fig. 4a and 4b, it is hard to believe that the two pictures correspond to the same JSD. This is due to the extremely high resolution offered by our technique: for each pixel of the SPDC graph we have more than 100 pixels in the DGF measurement. Thus, to verify that the difference in the two measurements is simply determined by the spectral resolution, we calculated the expected JSD in the two cases (see Fig. 4c and d and Supplementary Information I).

When we assume a resolution of 224 pm of the SPDC experiment, the calculated JSD (Fig. 4c) corresponds to the blurred blob obtained from the coincidence measurement (Fig. 4a). On the contrary, if the resolution is increased, the calculated JSD (Fig. 4d) is in excellent agreement with that revealed by the DFG measurements (Fig. 4b). It should be noted that the characteristic grid pattern is the result of interferences within the waveguide due to the high index mismatch at the waveguide facets. The resulting high reflectivity creates a Fabry-Perot cavity situation for both output modes, so that the final two-photon spectrum is shaped by the characteristic transmission functions of the signal and idler cavities (see Supplementary Information I). Interestingly, this effect was theoretically predicted for resonant SPDC devices four years ago [20], but it has *never* been observed, due to the limitations on the resolution of measurements made with single photon detectors. The high resolution JSD measurement presented here boosts the pixel count over the SPDC results by two orders of magnitude, while taking less than half as long to collect.

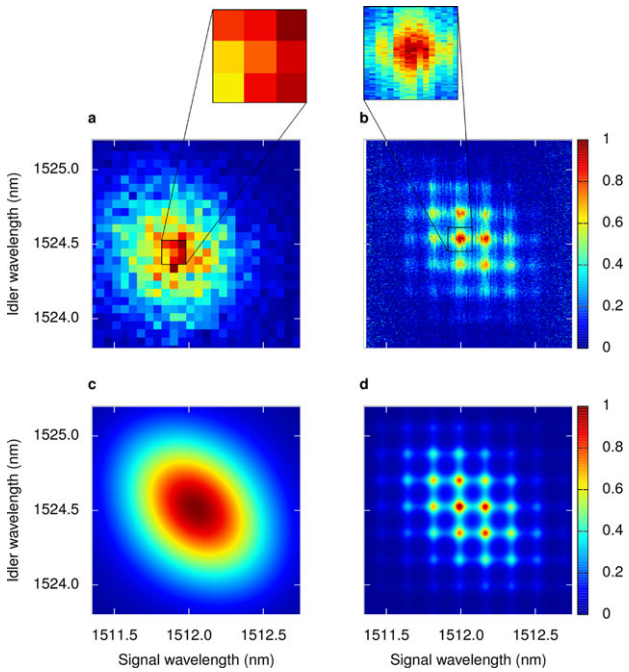

Figure 4 Results: (a) Experimental JSD obtained by SPDC-based measurements (see Fig. 2) with a sampling rate of 25 × 25 pixels over 1.4 nm × 1.4 nm, an integration time of 120 min, and a spectral resolution of 224 pm. The pixel pitch of 56 pm × 56 pm is determined by the group velocity dispersion of the DCF coils and the temporal resolution of the TDC to measure photon arrival times. (b) Experimental JSD obtained by DFG-based measurements (see Fig. 3) with a sampling rate of 141 × 501 pixels over 1.4 nm × 1.4 nm, an integration time of 45 min, and a spectral resolution of 20 pm. The pixel pitch of 10 pm × 2.8 pm corresponds to the scanning steps of the seed laser on the x-axis and to the spectral span over the number of data points of the OSA on the y-axis. The raw spectral data has been normalized to account for varying seed power (see Methods), leading to increased noise levels towards the left and the right edge of the plot. The visible offset between SPDC and DFG central wavelengths is caused by a shift of the central pump wavelength by 0.1 nm when re-locking the pump laser. (c) The figure c) is the convolution of figure d) with a Gaussian of FWHM 224pm, corresponding to the resolution of the SPDC measurement. (d) Numerical calculation of the SPDC photon pairs' JSD generated by the device under study.

Thanks to this dramatic increase in data acquisition rate, it becomes possible to fully exploit the spectral resolution of the seed laser and the detector, and at the same time minimize statistical errors within realistic measurement durations.

Assuming a pure pump state, the Schmidt number $K = 1.05$ (obtained from simulations) quantifies the spectral entanglement of SPDC photon pairs emitted by the sample [21, 22]. From the measured high resolution JSD (Fig. 4b), we can under this assumption estimate an experimental lower boundary [23] at $K_{\min}^{\exp} = 1.04$ after noise suppression, corresponding to a theoretical value of $K_{\min} = 1.03$ extracted from (Fig. 4d) (see Supplementary Information II).

3. Experimental parameters

Figures 2 and 3 depict the measurement set-ups for the direct reconstruction of the JSD for SPDC and DFG-based methods, respectively. In each experiment, the sample is pumped by a mode-locked Coherent Mira Ti:Sapphire picosecond pulse laser at 759.1 nm, with a 0.4 nm spectral FWHM. Its repetition rate is reduced from 76 MHz to 3.8 MHz with an APE Pulse Select acousto-optical pulse picker, introducing a temporal jitter of up to $\tau_{\mathrm{PP}} = 200$ ps into the pump laser's trigger signal. The beam power in front of the waveguide is 46 mW.

The sample is a chemically-etched ridge AlGaAs waveguide grown by molecular-beam epitaxy. The employed phasematching scheme is non-collinear with a pump pulse impinging on top of the waveguide at almost perpendicular incidence [13]. Signal and idler beam are emitted in cross-polarized, counterpropagating modes from either of two simultaneously phase-matched type II SPDC processes [19] (see Supplementary Information I for details).

In SPDC measurements, both signal and idler photons are collected on either side of the source with X40 microscope objectives. A set of wave plates and a polarizer allow us to select the correct polarization mode for each photon. Both photons then travel through DCF spools with a dispersion of $D_{\mathrm{DCF}} = -1475$ ps/nm. Free-running idQuantique id220 avalanche photo diodes (APD) act as single photon detectors at the end of each fiber. Detection efficiency is set to 20%, the timing jitter of the electrical detection signal is $\tau_{\mathrm{APD}} = 250$ ps and the dead time $\tau_p = 10$ µs. A quTools quTau TDC, connected to the APDs, measures the photons' arrival times relative to the pump laser's electrical trigger pulse with a $\tau_{\mathrm{TDC}} = 81$ ps mean temporal bin size. The spectral resolution of the fiber spectrometer assembly is given by the joint temporal jitter of the pulse picker and the APD, as well as the TDC time resolution over DCF dispersion, resulting in $\Delta\lambda_{\mathrm{SPDC}} = \sqrt{\tau_{\mathrm{PP}}^2 + \tau_{\mathrm{APD}}^2 + \tau_{TDC}^2}/D_{\mathrm{DCF}} = 224$ pm. The brightest "pixel" contains exactly 100 coincidence counts, so that detector saturation or multiple photon pair events distorting the result spectrum are not an issue.

In DFG measurements, we use a Yokogawa 6730C OSA with a resolution of 20 pm for spectral analysis of the idler beam. We employ a Tunics-Plus CW laser with a line-width of 100 kHz at an output power level of 8 mW to stimulate downconversion. The tunable fibered Fabry-Perot filter TFFP from ozOptics was used to clean the seed laser line; it has a Gaussian transmission profile with a 1.1 nm FWHM set to be centered at 1512.1 nm. At the output facet of the waveguide less than 10% of the nominal seed power exits, mainly due to losses in the filter and coupling losses. With the help of the OSA, we detected a deviation from the nominal output wavelength by −0.33 nm and verified its relative wavelength accuracy to be within the OSA resolution. The

filter causes a variable seed laser power during the seed laser's wavelength sweep, which we monitored by recording the power P_{ref} of the seed beam exiting the waveguide and accounted for in Fig. 4b by dividing the experimental value for each data point by the corresponding seed beam power. The maximal total DFG power measured with the OSA was 290 nW.

4. Conclusion and outlook

We have implemented a novel technique to reconstruct the joint spectral density of biphoton states that would be emitted by spontaneous parameteric processes, using a completely classical difference frequency generation experiment. It significantly out-performs spectrally resolved single photon coincidence measurements, both in measurement time and resolution, and constitutes a fast, accurate, and reliable tool for the characterization of photon pair sources. Even in the first implementation performed here it provides a qualitative advance over previous methods, and reveals details of the biphoton joint spectral density that have never been observed before. Further enhancements can easily be achieved, as the 20 pm spectral resolution in our experiments could be improved by an order of magnitude using state-of-the-art spectrum analyzers and lasers. Adapting our method to explore polarization or spatial degrees of freedom would allow the complete characterization of biphoton states generated by parametric processes, opening the way to a new generation of experiments to explore hitherto unstudied aspects of nonclassical states of light.

Acknowledgement. M.L. was supported by the Italian Ministry of University and Research, FIRB Contract No. RBFR08XMVY, by the Fundation Alma Mater Ticinensis. J.S. was supported by the Natural Sciences and Engineering Research Council of Canada. This work was partly supported by the French Brazilian ANR HIDE project and by Région Ile de-France in the framework of C'Nano IdF with the TWILIGHT project. S.D acknowledges the Institut Universitaire de France.

Supporting Information: for this article is available free of charge under http://dx.doi.org/10.1002/lpor.201400057

Received: 13 March 2014, **Revised:** 7 May 2014,
Accepted: 20 May 2014

Published online: 25 June 2014

Key words: Photon pair sources, nonlinear optics, spectral correlations, semiconductor photonics.

References

[1] Z. Yang, M. Liscidini, and J. E. Sipe, Phys. Rev. A **77**(3), 033808 (2008).
[2] Y. H. Kim and W. P. Grice, Optics Letters **30**(8), 908 (2005).
[3] W. Wasilewski, P. Wasylczyk, P. Kolenderski, K. Banaszek, and C. Radzewicz, Optics Letters **31**(8), 1130 (2006).
[4] M. Avenhaus, A. Eckstein, P. J. Mosley, and C. Silberhorn, Opt. Lett. **34**(18), 2873–2875 (2009).
[5] J. L. O'Brien, A. Furusawa, and J. Vučković, Nature Photon. **3**(12), 687 (2009).
[6] E. Martín-López, A. Laing, T. Lawson, R. Alvarez, X. Q. Zhou, and J. L. O'Brien, Nature Photon. **6**(11), 773 (2012).
[7] W. J. Munro, A. M. Stephens, S. J. Devitt, K. A. Harrison, and K. Nemoto, Nature Photon. **6**(11), 777 (2012).
[8] M. A. Broome, A. Fedrizzi, S. Rahimi-Keshari, J. Dove, S. Aaronson, T. C. Ralph, and A. G. White, Science **339**(6121), 794 (2013).
[9] A. Crespi, R. Osellame, R. Ramponi, D. Brod, E. Galvão, N. Spagnolo, C. Vitelli, E. Maiorino, P. Mataloni, and F. Sciarrino, Nature Photon. **7**(7), 545–549 (2013).
[10] M. Collins, C. Xiong, I. Rey, T. Vo, J. He, S. Shahnia, C. Reardon, T. Krauss, M. Steel, A. Clark, and B. Eggleton, Nature Communications **4**, 2582 (2013).
[11] L. G. Helt, M. Liscidini, and J. E. Sipe, J. Opt. Soc. Am. B **29**(8), 2199 (2012).
[12] E. J. Mason, M. A. Albota, F. König, and F. N. C. Wong, Opt. Lett. **27**(23), 2115 (2002).
[13] X. Caillet, V. Berger, G. Leo, and S. Ducci, J. Mod. Opt. **56**(2–3), 232–239 (2009).
[14] S. Azzini, D. Grassani, M. Galli, L. C. Andreani, M. Sorel, M. J. Strain, L. G. Helt, J. E. Sipe, M. Liscidini, and D. Bajoni, Opt. Lett. **37**(18), 3807 (2012).
[15] F. De Martini, V. Bužek, F. Sciarrino, and C. Sias, Nature **419**(6909), 815–818 (2002).
[16] M. Liscidini and J. E. Sipe, Phys. Rev. Lett. **111**(Nov), 193602 (2013).
[17] J. Chen, A. J. Pearlman, A. Ling, J. Fan, and A. L. Migdall, Opt. Express **17**(8), 6727 (2009).
[18] T. Gerrits, M. J. Stevens, B. Baek, B. Calkins, A. Lita, S. Glancy, E. Knill, S. W. Nam, P. R. Mirin, R. H. Hadfield, R. S. Bennink, W. P. Grice, S. Dorenbos, T. Zijlstra, T. Klapwijk, and V. Zwiller, Opt. Express **19**(24), 24434 (2011).
[19] A. Orieux, A. Eckstein, A. Lemaître, P. Filloux, I. Favero, G. Leo, T. Coudreau, A. Keller, P. Milman, and S. Ducci, Phys. Rev. Lett. **110**(16), 160502 (2013).
[20] Y. Jeronimo-Moreno, S. Rodriguez-Benavides, and A. U'Ren, Laser Phys. **20**(5), 1221–1233 (2010).
[21] R. Grobe, K. Rzazewski, and J. H. Eberly, J. Phys. B **27**(16), L503 (1994).
[22] C. K. Law, I. A. Walmsley, and J. H. Eberly, Phys. Rev. Lett. **84**(Jun), 5304–5307 (2000).
[23] G. Harder, V. Ansari, B. Brecht, T. Dirmeier, C. Marquardt, and C. Silberhorn, Opt. Express **21**(12), 13975 (2013).